Carbohydrate Polymers 97 (2013) 45–51

Contents lists available at SciVerse ScienceDirect

Carbohydrate Polymers

journal homepage: www.elsevier.com/locate/carbpol

Studies on the structure of coumarin-modified dextran nanoparticles by fluorescence spectroscopy

Holger Wondraczek[a,1], Anne Kotiaho[b,*], Marja Niemi[c], Pedro Fardim[a,1], Thomas Heinze[a,d,**,1]

[a] Laboratory of Fibre and Cellulose Technology, Åbo Akademi University, Porthansgatan 3, 20500 Åbo, Finland
[b] Nanoscience Center, Department of Chemistry, P.O. Box 35, 40014 University of Jyväskylä, Finland
[c] Tampere University of Technology, P.O. Box 541, 33101 Tampere, Finland
[d] Center of Excellence for Polysaccharide Research, Institute of Organic Chemistry and Macromolecular Chemistry, Friedrich Schiller University of Jena, Humboldtstraße 10, D-07743 Jena, Germany

ARTICLE INFO

Article history:
Received 8 December 2012
Accepted 12 April 2013
Available online 25 April 2013

Keywords:
Polysaccharide nanoparticles
UV–vis spectroscopy
Coumarin
Time-resolved fluorescence spectroscopy
Photoactivity

ABSTRACT

The photophysical and photochemical characteristics of nano-scaled particles obtained via solvent displacement from coumarin-modified dextrans were studied by means of absorption- and fluorescence-spectroscopy. The environment-dependent fluorescence emission of the pendant 4-methyl-7-alkoxy coumarin groups was exploited as a probe to gain information about the inner structure of the polysaccharide based nanoparticles. Time-resolved fluorescence measurements showed that the particles had two domains of different polarity and it could be confirmed that the core of the nano-assemblies contained water. Moreover, preliminary experiments were carried out demonstrating the possibility to control the morphology of the nanoparticles by the light induced $2\pi + 2\pi$ cycloaddition of the coumarin substituents.

1. Introduction and scope

Recently, polymeric nanoparticles based on polysaccharide derivatives with high degree of substitution (DS) have received much attention due to their biocompatibility, enormous structural diversity, and functional versatility (Bachelder, Beaudette, Broaders, Dashe, & Frechet, 2008; Bachelder et al., 2010; Beaudette et al., 2009; Broaders, Grandhe, & Frechet, 2011; Cohen et al., 2010, 2011; Cui, Cohen, Broaders, Beaudette, & Frechet, 2011; Hornig et al., 2008; Hornig & Heinze, 2008; Hornig, Heinze, Hesse, & Liebert, 2005; Liebert, Hornig, Hesse, & Heinze, 2005; Wondraczek, Elschner, & Heinze, 2011). However, it is obvious that knowledge of the structure and of the local microenvironment inside the polysaccharide particles is of fundamental importance for any of the desired applications. Therefore, fluorescent probe molecules, whose fluorescence properties characterize their distinct environment, have been commonly employed to investigate the structure of organized assemblies. In earlier studies on nanoparticles of hydrophobic polysaccharide derivatives with low DS, pyrene has been incorporated into gel-particles and it has been concluded that the particles contain hydrophobic domains in the core and a hydrophilic shell (Akiyoshi, Deguchi, Moriguchi, Yamaguchi, & Sunamoto, 1993; Lee, Jo, Kwon, Kim, & Jeong, 1998; Nishikawa, Akiyoshi, & Sunamoto, 1994; Vieira, Moscardini, Tiera, & Tiera, 2003; Yinsong, Lingrong, Jian, & Zhang, 2007). In the case of polysaccharide derivatives with a high DS, hydrophobic domains have been also confirmed in fluorescence probe studies (Hornig & Heinze, 2007). Although fluorophores can be entrapped in nanoparticles, their covalent attachment to the particle forming polymer would offer various advantages: the fluorophores are fixed to the particles, preventing leaching, the polysaccharide matrix can prevent fluorescence quenching often caused by high concentration of fluorophores, and the fluorophores are uniformly distributed in the interior of the macromolecular assembly. Moreover, the inner structure of the particles will not be affected by the incorporation of the additional probe itself.

Recently, 4-methyl-7-alkoxy coumarin molecules were used as hydrophobic modifiers for nanoparticle-forming polysaccharide derivatives in order to control the particle properties utilizing the photo-active character of this type of chromophores (Wondraczek & Heinze, 2008). However, coumarins are also applicable as fluorescent probes since their fluorescence properties are sensitive to the polarity of their microenvironment (Wagner, 2009). 7-Alkoxy

* Corresponding author. Tel.: +358 40 8054442.
** Principal corresponding author at: Center of Excellence for Polysaccharide Research, Institute of Organic Chemistry and Macromolecular Chemistry, Friedrich Schiller University of Jena, Humboldtstraße 10, D-07743 Jena, Germany. Tel.: +49 3641 9 48270; fax: +49 3641 9 48272.
E-mail addresses: anne.m.kotiaho@jyu.fi (A. Kotiaho), thomas.heinze@uni-jena.de (T. Heinze).
[1] Member of EPNOE.

0144-8617/$ – see front matter © 2013 Elsevier Ltd. All rights reserved.
http://dx.doi.org/10.1016/j.carbpol.2013.04.040

coumarins in particular exhibit a higher fluorescent quantum yield and fluorescence lifetime in a polar environment compared to a less polar one (Aaron et al., 1995; Heldt, Heldt, Ston, & Dieh, 1995; Muthuramu & Ramamurthy, 1984). In the present study we focus on the absorption and fluorescence properties of nanoparticles prepared from coumarin-modified dextran derivatives with different DS. Fluorescence lifetime measurements were applied to get more information about the particle structure and morphology.

2. Experimental

2.1. Materials

N,N-Dimethylacetamide (DMAc) was purchased from Sigma–Aldrich (purity 99%). Deionized water was obtained from a Millipore Milli-Q system. Photoactive dextran derivatives (dextran [(4-methyl-2-oxo-2H-chromen-7-yl)oxy] acetate) were synthesized as described elsewhere(Wondraczek & Heinze, 2008). Nanoparticles were prepared by dialysis. Briefly, the dextran derivative (20 mg) was dissolved in DMAc (5 mL) and dialyzed against deionized water (400 mL) using a regenerated cellulose dialysis membrane (Spectra/Por, molecular weight cut off of 3500 g/mol). The water was first renewed after at least 12 h and then subsequently four times after at least 3 h.

2.2. Characterization methods

The hydrodynamic diameter of the nanoparticles was determined by dynamic light scattering using a Malvern zetasizer Nano ZS instrument (He–Ne laser 633 nm, scattering angle: 173°). The mean particle size was approximated as the effective (*Z*-average) diameter and the width of the distribution as the polydispersity index (PDI). Both parameters were achieved using the cumulants method for data analysis, assuming spherical particle shape and log-normal size distribution. The effective zeta-potential of the nanoparticles was determined by electrophoretic light scattering (ELS) using a Malvern zetasizer Nano ZS instrument. It was calculated using the Smoluchowski equation. The measurements were repeated three times for each sample. The intrinsic error of the measured zeta-potential was ±5 mV.

Extinction (absorption + scattering) spectra of the aqueous particle suspensions were measured using a Perkin-Elmer λ900 spectrophotometer equipped with an integrating sphere (PELA-1000). The sample cuvette (optical path 10 mm) was placed at the beam entrance of the integrating sphere. This setup reduces the effect from scattering of light by the nanoparticles significantly and thus the measured spectra are referred to as absorption spectra (Merzlyak & Naqvi, 2000), even though this is not the absorption in the physical correct sense. Fluorescence spectra of the aqueous nanoparticle suspensions were measured using a Perkin-Elmer LS50B spectrofluorometer. A time-correlated single photon counting (TCSPC) system consisting of a PicoHarp 300 controller and a PDL 800-B driver was used for the time resolved fluorescence measurements. The excitation wavelength was 340 nm from a pulsed diode laser head PLS-8-2-295. The fluorescence signal was detected with a micro channel plate photomultiplier (Hamamatsu R2809U). The time resolution of the instrument was approximately 320 ps (full width, half maximum). The fluorescence decays were fitted to a multiexponential model, from which an amplitude-weighted fluorescence lifetime was calculated. The decay associated spectra were obtained by measuring the decay curve at each monitoring wavelength with a constant data accumulation time and fitting the decays globally. The amplitudes were corrected by taking into account the wavelength sensitivity of the photomultiplier tube. The amplitudes at <390 nm may appear lower compared to the actual values, because an optical filter with a sharp change in transmittance at 380 nm was used for excluding the excitation light from the detector. The stability of the samples during DAS measurements was monitored by measuring the absorption spectra before and after the experiments.

Table 1
Size, polydispersity index (PDI), and zeta-(ζ)-potential of nanoparticles prepared from dextran [(4-methyl-2-oxo-2H-chromen-7-yl)oxy] acetate depending on the degree of substitution (DS).

DS[a]	Diameter [nm]	PDI	ζ-potential [mV]
0.44	314	0.135	−25
0.94	218	0.145	−31
1.63	182	0.124	−30
2.32	131	0.093	−38

[a] Determined by ^{1}H NMR spectroscopy (Wondraczek & Heinze, 2008).

3. Results and discussion

Coumarin-modified dextran was prepared by the reaction of the biopolymer with [(4-methyl-2-oxo-2H-chromen-7-yl)oxy]acetic acid activated by *N,N′*-carbonyldiimidazole. It was transferred to nanoparticles by an exchange of the organic solvent DMAc against the non-solvent water (Fig. 1) (Wondraczek & Heinze, 2008). The diameter of the coumarin-modified dextran nanoparticles was in the range from 131 to 314 nm and it decreases with increasing DS (Table 1). All particles obtained possess a negative zeta-(ζ)-potential and thus the stability of the suspension can be attributed to electrostatic repulsion.

The suspensions of the particles obtained by dialysis (estimated concentration of particles 1 mg/mL) were adjusted to contain approximately equal amounts of polysaccharide derivative by diluting them to 2% (v/v), thus making it possible to compare the

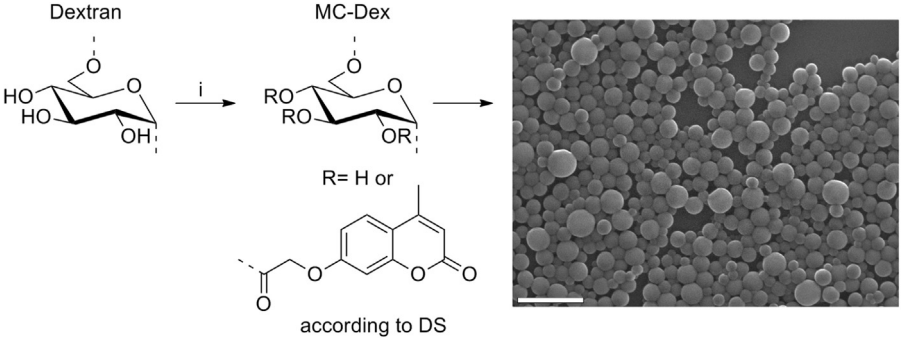

Fig. 1. Synthesis of 4-methyl-7-alkoxy coumarin functionalized dextran (MC-Dex) and SEM picture of nanoparticles obtained via solvent exchange (scale bar is 1 μm): (i) [(4-methyl-2-oxo-2H-chromen-7-yl)oxy]acetic acid, *N,N*-carbonyldiimidazole, DMSO, 16 h, 80°C.

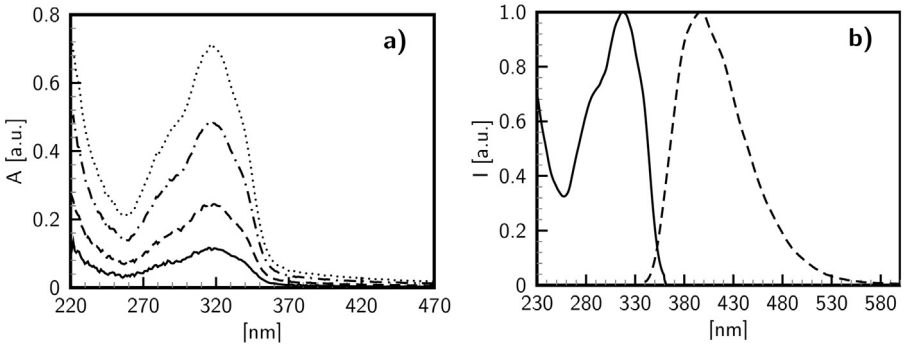

Fig. 2. (a) Absorption spectra of nanoparticle suspensions in water: degree of substitution (DS) 0.44 (solid line), DS 0.94 (dash), DS 1.63 (dot-dash) and DS 2.32 (dot). The suspensions obtained from dialysis were diluted to 2 vol%. (b) Fluorescence emission- (λ_{ex}=320 nm, dashed line) and excitation spectra (λ_{em}=320 nm, solid line) of nanoparticles with DS of 2.32.

absorbance values between different samples. The absorption spectra of the particles show the typical $\pi \rightarrow \pi^{*1}B$ transition below 250 nm, the $\pi \rightarrow \pi^{*1}L_a$ transition as a shoulder at 290 nm, and $\pi \rightarrow \pi^{*1}L_b$ transition with a maximum at 320 nm (Fig. 2a) (Song & Gordon, 1970). The absorbance increases with increasing DS, which is reasonable since there are more coumarin moieties for the same amount of polymer. The wavelength of maximum absorption is the same (≈320 nm) for particles of low DS values and slightly blue-shifted (317 nm) for particles with the highest DS of 2.32. The fluorescence emission spectrum of the particles with a DS of 2.32 is shown in Fig. 2b. The spectra of particles of different DS are qualitatively similar possessing a maximum at 397–400 nm. A comparison of the fluorescence intensities of different particle samples was not considered reliable because of scattering. The fluorescence excitation spectra of particles with a DS of 0.44 and 2.32 have a maximum at 320 and 317 nm, respectively. The comparison of the absorption- and fluorescence-excitation spectra indicates that the setup with the integrating sphere produces precise results in the case of the smallest particles, but as the particle size increases the scattering causes minor differences between the absorption and fluorescence excitation spectra.

As pointed out, the fluorescence spectra of the different particle suspensions could not give a reliable comparison of fluorescence efficiencies of the particles with varying DS because of their different scattering properties. Therefore, the fluorescence decays were measured and as can be noticed from the direct comparison of the particles prepared from the dextran derivatives with a DS of 0.44 and 2.32, respectively (Fig. 3a), the decay becomes faster as the DS increases. An optimal fit (minimized χ^2) of the decays according to

$$I(t) = a_0 + \sum_{i=1}^{n} a_i\, e^{(-t/\tau_i)}$$

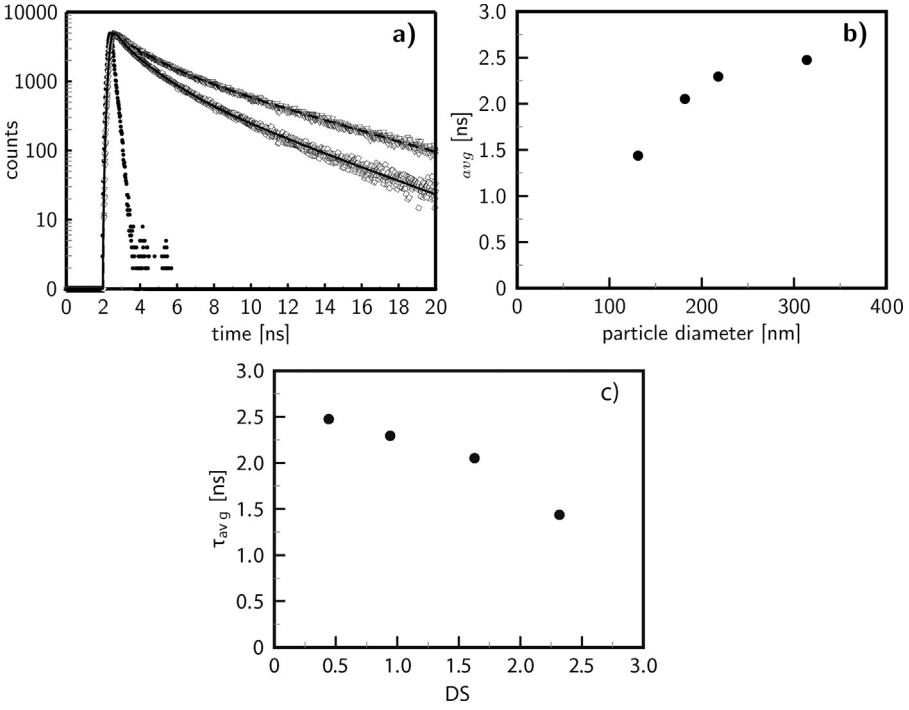

Fig. 3. (a) Fluorescence decay curves and their 3-exponential fits of particles obtained via dialysis from dextran 2-[(4-methyl-2-oxo-2*H*-chromen-7-yl)oxy] acetates with a DS of 0.44 (triangles, dashed line) and DS 2.32 (squares, solid line), instrumental response shown as dots; (b) amplitude-weighted fluorescence lifetime as function of the of particle diameter and (c) the degree of substitution (DS).

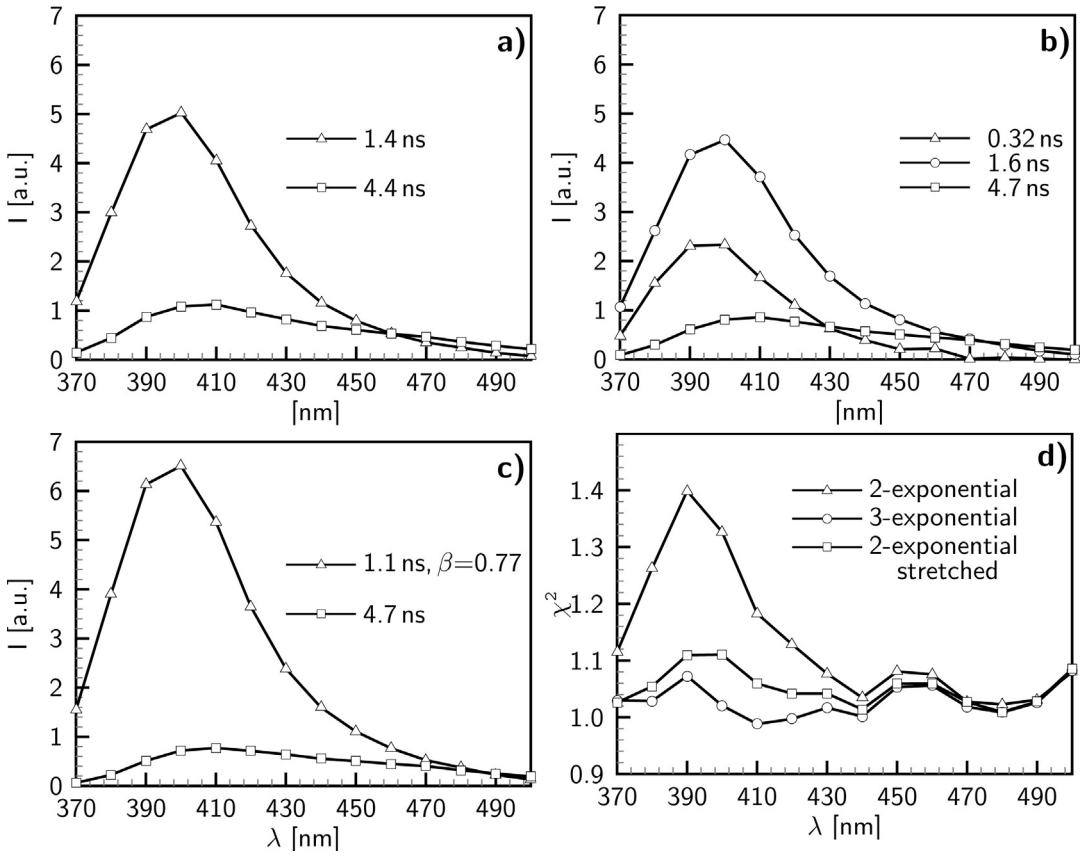

Fig. 4. Decay associated fluorescence spectra of particles obtained via dialysis from dextran 2-[(4-methyl-2-oxo-2*H*-chromen-7-yl)oxy] acetate with a DS 2.32: data analysis via (a) two-exponential fit, (b) three-exponential fit, and (c) two-exponential fit, where the shorter component is fitted with a stretched exponential; (d) weighted mean square deviation of the fits presented in (a-c).

requires a 3-exponential model and the amplitude-weighted fluorescence lifetime ($\langle\tau\rangle$) that was calculated according to:

$$\langle\tau\rangle = \frac{\sum_{i=1}^{3} a_i \tau_i}{\sum_{i=1}^{3} a_i}$$

As shown in Fig. 3b and c, the amplitude-weighted fluorescence lifetime decreases moderately from 2.5 to 1.5 ns with increasing DS (0.44–2.32) or decreasing particle size (314–131 nm).

Two factors are known from literature that can cause a severe decline in the fluorescence quantum yield or lifetime of 7-alkoxy coumarins: aggregation in solid state and less polar environment compared to water (Aaron et al., 1995; Fery-Forgues, Cantuel, & Fournier-Noel, 2010; Heldt et al., 1995; Muthuramu & Ramamurthy, 1984). Since dextran is a hydrophilic polysaccharide, possessing three hydroxyl groups per repeating unit, some relatively polar domains might be provided by the polymer backbone, especially in the particles prepared from derivatives with low DS. The modification of the hydroxyl groups with the hydrophobic chromophores decreases the hydrophilicity of the resulting derivative and increases the concentration of coumarin moieties. Thus, a decrease of 7-alkoxy coumarin fluorescence lifetime with increasing DS of the dextran derivative seems reasonable. However, it is important to note that a high increase of the coumarin DS, from 0.44 to 2.32 does not decrease the amplitude-weighted fluorescence lifetime excessively. This indicates that a high amount of coumarins can be incorporated in the particles without the loss of fluorescent properties. Moreover, it needs to be emphasized that the amplitude-weighted fluorescence lifetimes determined in case of the dextran 2-[(4-methyl-2-oxo-2*H*-chromen-7-yl)oxy] acetate nanoparticles are in the range of the lifetime of the low molecular weight model compound 7-methoxy-4-methyl-2*H*-chromen-2-one in water ($\tau \approx 1.8$ ns).

The 3-exponential model used for the fit of the fluorescence decays is useful in obtaining the amplitude-weighted fluorescence lifetime. However, assigning three discrete fluorescence lifetimes in a physically significant way is difficult. Thus, decay associated spectra from the particle suspensions were established by measuring the intensity decay across the whole emission spectra, in order to get more information on the nature of the emitting coumarin species. The results obtained from the measurements of the particle suspension obtained from the dextran derivative with a DS of 2.32 will be discussed as a representative example. It turned out clearly that the fluorescence decays $I(\lambda, t)$ are not monoexponential. Therefore, different fits according to

$$I(\lambda, t) = \sum_{i}^{n} a_i(\lambda) e^{(-t/\tau_i)}$$

were tested with respect to two criteria: fit quality in terms of weighted mean square deviation (χ^2) and the meaningfulness of the fit. The values of χ^2 should be as close as possible to one and here values <1.2 were considered to be acceptable. The two-exponential fit results in two components with fluorescence lifetimes of 1.4 and 4.4 ns (Fig. 4a), but this fit is of poor quality (Fig. 4d). The fit quality is improved by adding a third exponential, and a further increase in the number of exponentials did not improve the fit quality significantly. In the case of the three-exponential fit, the spectra of the components with shorter lifetimes (<0.32 and 1.6 ns) have very similar shapes. In addition, though the polymer and particle environment is expected to alter the fluorescence lifetime of

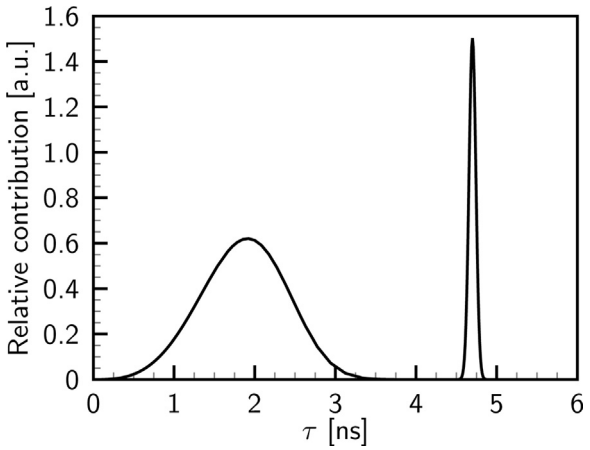

Fig. 5. Fluorescence lifetime distribution of particles obtained via dialysis from dextran 2-[(4-methyl-2-oxo-2*H*-chromen-7-yl)oxy] acetate with a DS 2.32 calculated on basis of two-exponential fit, where the shorter component is fitted with a stretched exponential (τ = 1.1 ns, β = 0.77) and the longer component is illustrated with a Gaussian (full width, half maximum 0.1 ns). The relative areas of the shorter and longer components were set as 0.84 and 0.16, respectively.

the coumarin molecules, three distinct lifetimes (or environments) are difficult to define. A more reasonable assumption is that the two components with shorter lifetimes obtained from the three-exponential fit are actually presenting the same fluorescent species, which are located in an environment of varying polarity. Therefore, a stretched exponential, $e^{(-t/\tau)^{\beta}}$, was used to describe a lifetime distribution (Berberan-Santos, Bodunov, & Valeur, 2005). In this model the stretching parameter β estimates homogeneity of the environment of the fluorophores. The model returns to exponential when $\beta = 1$, and with decreasing values of β the lifetime distribution becomes broader. Fitting the data only with stretched exponential results in a very poor fit quality, but a combination of a stretched exponential decay for the shorter lifetime and an exponential decay for the longer lifetime according to

$$I(t) = a_1 \cdot e^{(-t/\tau_1)^{\beta}} + a_2 \cdot e^{(-t/\tau_2)}$$

yields almost the same fit quality as in case of the 3-exponential model (Fig. 4d). Attempts to include a distribution in the longer lifetime did not result in significant improvements of the fit and thus were omitted. The resulting decay associated spectra (Fig. 4c) reveal two components with lifetimes of 1.1 ns (β = 0.77) and 4.7 ns. Since the spectra of the two components have different shapes, two different fluorescent species are confirmed in the particles, or in other words, the 2-[(4-methyl-2-oxo-2*H*-chromen-7-yl)oxy] acetate chromophores are located in two different microenvironments. One of these microenvironments has a very well defined polarity and the other one has varying polarity.

For a numerical analysis, the distribution of the lifetime was calculated from the rate probability density function and its asymptotic form obtained by the saddle-point method (Zatryb, Podhorodecki, Misiewicz, Cardin, & Gourbilleau, 2011):

$$\Phi(k) = \frac{\alpha\tau}{\sqrt{2\pi k}} \cdot (k\tau)^{[-1/(-\alpha/2)]} \cdot e^{[-(k\tau)^{-\alpha}]} \quad \text{with} \quad \alpha = \frac{\beta}{1-\beta}$$

$$\text{and} \quad \tau = \frac{\tau_0}{\beta(1-\beta)^{(1/\alpha)}}$$

After the rate distribution is obtained, it can be converted to the lifetime distribution by taking the inverse of the rate. The lifetime distribution calculated using the values τ_0 = 1.1 ns and β = 0.77 is shown in Fig. 5. The distribution of the 4.7 ns lifetime is illustrated by approximating the very narrow distribution of a lifetime obtained from mono-exponential decay with a Gaussian (full width, half maximum 0.1 ns).

Keeping in mind the lifetime of the low molecular weight model compound 7-methoxy-4-methyl-2*H*-chromen-2-one (τ = ≈1.8 ns in water and τ = ≈0.3 ns in DMSO), it can be concluded that that the fluorophores accounting for the 1.1 ns component face a lower polarity compared to water, but yet a highly polar environment. Actually, with the distribution taken into account, the 1.1 ns component presents coumarins in a range of environments, varying from waterlike to relatively less polar. This indicates that the core of the nanoassemblies contains water, which might be included during the particle formation. The spectrum of the component with the longer lifetime (4.7 ns) is slightly red-shifted compared to that of the 1.1 ns component. As known from studies of the model compound (results not shown), an increase in polarity of the solvent yields a red-shift of the fluorescence. Another possible reason for red-shifted fluorescence would be excimer emission, which has been reported for coumarin derivatives linked to polymers and in cellulose based host-guest systems(Arici, Greiner, Hou, Reuning, & Wendorff, 2000; Chen & Hong, 1997). However, a broad excimer emission band would be expected to appear at wavelengths longer than 420 nm. Both the longer lifetime and the red-shift of the spectrum thus indicate that the 4.7 ns component belongs to coumarins in an environment of higher polarity compared to the ones with 1.1 ns lifetime. Unexpectedly, the lifetime of 4.7 ns exceeds the value measured for the model compound in water and thus needs to be assigned to chromophores located in an environment possessing charged groups. Since the negative ζ-potential (Table 1) suggests a negative surface charge, these chromophores can be assigned to the particle surface.

Summing up the fluorescence measurements described, it is possible to draw a tentative picture of the nanoparticles prepared via dialysis from dextran 2-[(4-methyl-2-oxo-2*H*-chromen-7-yl)oxy] acetates. It can be concluded from the decay associated spectra that the particles possess two domains with a medium (distributed) and a very high polarity. From the comparison of the lifetimes of the fluorescent species located in these domains with a low molecular weight model, it turned out that the chromophores at the surface face a polarity, which is higher than water. The shorter lifetime possess a distribution indicating that the corresponding chromophores are located in environment of a polarity varying form relatively unpolar to waterlike. Therefore, the simple model of a hydrophilic shell and a hydrophobic core suggested by previous studies needs to be reconsidered (Hornig & Heinze, 2007). Moreover, the combination of ζ-potential- and the fluorescence lifetime measurements indicates the presence of charged groups at the surface. On the basis of the current knowledge, the origin of these charges can not be explained by the molecular structure of the particle forming polymer. Therefore, a detailed study on the surface chemistry of the particles will be carried out and reported elsewhere.

Beside the investigation of the particle morphology, preliminary experiments regarding the crosslinking of polymer chains in the particles via photoinduced $2\pi + 2\pi$ cycloaddition of the pendant 2-((4-methyl-2-oxo-2*H*-chromen-7-yl)oxy) acetate moieties were carried out. Fig. 6 shows the fluorescence spectra of particles obtained via dialysis from dextran 2-[(4-methyl-2-oxo-2*H*-chromen-7-yl)oxy] acetate with a DS of 2.32 before (solid line) and after 300 s of illumination at 333 nm (dashed line). The decrease of the fluorescence intensity proves the reaction of the fluorescent coumarin moieties to the non-fluorescent dimers Kehrloesser, Baumann, Kim, and Hampp (2011). Moreover, a blue-shift of 13 nm of the fluorescence band is observed. This indicates that the species emitting at longer wavelengths have lost their fluorescence intensity. Taking into account the decay associated spectra measured and the related structural model proposed, the coumarin moieties in

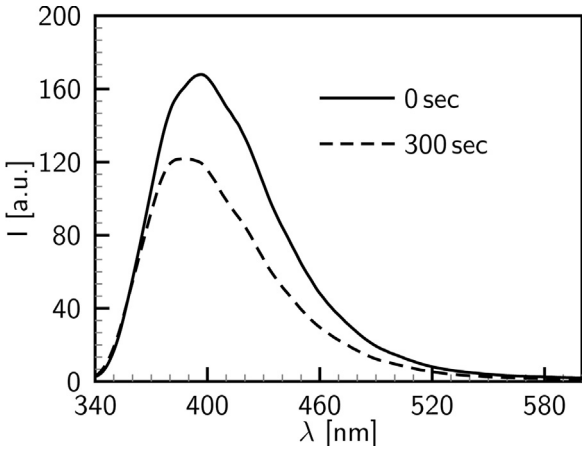

Fig. 6. Fluorescence spectra (λ_{ex} = 320 nm) of particles obtained via dialysis from dextran 2-[(4-methyl-2-oxo-2*H*-chromen-7-yl)oxy] acetate with a DS of 2.32 before (solid line) and after 300 s of illumination at 333 nm (dashed line).

the polar domains at the surface are preferably crosslinked, which is seen as a blue-shift in fluorescence spectrum. This means, it is possible to control the chemical nature of the particles at the nanoscale. Interestingly, the particle properties, which are accessible by dynamic light scattering (size and ζ-potential) remain constant during the irradiation.

4. Conclusions

Fluorescence studies of coumarin-containing polysaccharide nanoparticles indicate that the absorption spectra of the light-scattering particle suspensions measured using an integrating sphere correspond well to the fluorescence excitation spectra. The absorption spectra show the typical coumarin bands and the absorbance is higher for the particles prepared from dextran derivatives with a higher DS of coumarin moieties. The shape of the fluorescence spectrum was not much affected by the DS. The fluorescence lifetime measurements indicate that higher nanoparticle absorption can be achieved by increasing the DS of coumarins from 0.4 up to 2.3 without a major loss of fluorescence intensity (amplitude-weighted fluorescence lifetime decreased from 2.5 ns to 1.5 ns). The results of fluorescence lifetime measurements allow to draw a tentative picture of the particle morphology. The decay-associated fluorescence spectra of the particles can be described by a two-exponential model, where the coumarin fluorescence lifetime attributed to the core has a distribution indicating that its polarity varies form non-polar to waterlike. The second longer fluorescence lifetime can be assigned to the highly polar surface of the particles. Since the findings reported in this work indicate, that the core of the particles contains water, the simple model of a hydrophilic shell and a hydrophobic core suggested by previous studies needs to be reconsidered. However, further studies are required in order to fully confirm the nanoparticle structure suggested and in particular the surface chemistry of the particles needs to be researched in detail.

Acknowledgements

Finnish Funding Agency for Technology and Innovation (Tekes) and Thuringian Ministry for Education, Science and Culture (grant #B514-09051, NanoConSens) are acknowledged for funding. M.N. acknowledges Academy of Finland for funding. The authors acknowledge Laboratory of Physics at Åbo Akademi for use of fluorescence spectrometer and K.-M. Källman for his assistance. Prof. Helge Lemmetyinen is acknowledged for critical discussion on the manuscript.

References

Aaron, J.-J., Buna, M., Parkanyi, C., Antonious, M. S., Tine, A., & Cisse, L. (1995). Quantitative treatment of the effect of solvent on the electronic absorption and fluorescence spectra of substituted coumarins: Evaluation of the first excited singlet-state dipole moments. *Journal of Fluorescence*, *5*, 337–347.

Akiyoshi, K., Deguchi, S., Moriguchi, N., Yamaguchi, S., & Sunamoto, J. (1993). Self-aggregates of hydrophobized polysaccharides in water – formation and characteristics of nanoparticles. *Macromolecules*, *26*, 3062–3068.

Arici, E., Greiner, A., Hou, H. Q., Reuning, A., & Wendorff, J. H. (2000). Optical properties of guest host systems based on cellulose derivatives. *Macromolecular Chemistry and Physics*, *201*, 2083–2090.

Bachelder, E. M., Beaudette, T. T., Broaders, K. E., Dashe, J., & Frechet, J. M. J. (2008). Acetal-derivatized dextran: An acid-responsive biodegradable material for therapeutic applications. *Journal of the American Chemical Society*, *130*, 10494–10495.

Bachelder, E. M., Beaudette, T. T., Broaders, K. E., Frechet, J. M. J., Albrecht, M. T., Mateczun, A. J., et al. (2010). In vitro analysis of acetalated dextran microparticles as a potent delivery platform for vaccine adjuvants. *Molecular Pharmaceutics*, *7*, 826–835.

Beaudette, T. T., Cohen, J. A., Bachelder, E. M., Broaders, K. E., Cohen, J. L., Engleman, E. G., et al. (2009). Chemoselective ligation in the functionalization of polysaccharide-based particles. *Journal of the American Chemical Society*, *131*, 10360–10361.

Berberan-Santos, M. N., Bodunov, E. N., & Valeur, B. (2005). Mathematical functions for the analysis of luminescence decays with underlying distributions 1, kohlrausch decay function (stretched exponential). *Chemical Physics*, *315*, 171–182.

Broaders, K. E., Grandhe, S., & Frechet, J. M. J. (2011). A biocompatible oxidation-triggered carrier polymer with potential in therapeutics rid g-2796-2010. *Journal of the American Chemical Society*, *133*, 756–758.

Chen, Y., & Hong, R. T. (1997). Photopolymerization of 7, 7′-coumarinyl polymethylene dicarboxylates: Fluorescence and kinetic study. *Journal of Polymer Science Part A: Polymer Chemistry*, *35*, 2999–3008.

Cohen, J. A., Beaudette, T. T., Cohen, J. L., Brooders, K. E., Bachelder, E. M., & Frechet, J. M. J. (2010). Acetal-modified dextran microparticles with controlled degradation kinetics and surface functionality for gene delivery in phagocytic and non-phagocytic cells. *Advanced Materials*, *22*, 3593–3597.

Cohen, J. L., Schubert, S., Wich, P. R., Cui, L., Cohen, J. A., Mynar, J. L., et al. (2011). Acid-degradable cationic dextran particles for the delivery of sirna therapeutics. *Bioconjugate Chemistry*, *22*, 1056–1065.

Cui, L. N., Cohen, J. A., Broaders, K. E., Beaudette, T. T., & Frechet, J. M. J. (2011). Mannosylated dextran nanoparticles: A ph-sensitive system engineered for immunomodulation through mannose targeting rid g-2796-2010. *Bioconjugate Chemistry*, *22*, 949–957.

Fery-Forgues, S., Cantuel, M., & Fournier-Noel, C. (2010). Searching for fluorescent nanocrystals in aqueous solutions of 7-methoxycoumarin. *Dyes and Pigments*, *87*, 241–248.

Heldt, J. R., Heldt, J., Ston, M., & Dieh, H. A. (1995). Photophysical properties of 4-alkylcoumarin and 7-alkoxycoumarin derivatives – Absorption and emission-spectra, fluorescence quantum yield and decay time. *Spectrochimica Acta Part A-Molecular and Biomolecular Spectroscopy*, *51*, 1549–1563.

Hornig, S., Biskup, C., Graefe, A., Wotschadlo, J., Liebert, T., Mohr, G. J., et al. (2008). Biocompatible fluorescent nanoparticles for ph-sensoring. *Soft Matter*, *4*, 1169–1172.

Hornig, S., & Heinze, T. (2007). Nanoscale structures of dextran esters. *Carbohydrate Polymers*, *68*, 280–286.

Hornig, S., & Heinze, T. (2008). Efficient approach to design, stable water-dispersible nanoparticles of hydrophobic cellulose esters. *Biomacromolecules*, *9*, 1487–1492.

Hornig, S., Heinze, T., Hesse, S., & Liebert, T. (2005). Novel nanoparticles based on dextran esters with unsaturated moieties. *Macromolecular Rapid Communications*, *26*, 1908–1912.

Kehrloesser, D., Baumann, R.-P., Kim, H.-C., & Hampp, N. (2011). Photochemistry of coumarin-functionalized SiO_2 nanoparticles. *Langmuir*, *27*, 4149–4155.

Lee, K. Y., Jo, W. H., Kwon, I. C., Kim, Y. H., & Jeong, S. Y. (1998). Structural determination and interior polarity of self-aggregates prepared from deoxycholic acid-modified chitosan in water. *Macromolecules*, *31*, 378–383.

Liebert, T., Hornig, S., Hesse, S., & Heinze, T. (2005). Nanoparticles on the basis of highly functionalized dextrans. *Journal of the American Chemical Society*, *127*, 10484–10485.

Merzlyak, M. N., & Naqvi, K. R. (2000). On recording the true absorption spectrum and the scattering spectrum of a turbid sample: Application to cell suspensions of the cyanobacterium anabaena variabilis. *Journal of Photochemistry and Photobiology B-biology*, *58*, 123–129.

Muthuramu, K., & Ramamurthy, V. (1984). 7-alkoxy coumarins as fluorescence probes for microenvironments. *Journal of Photochemistry*, *26*, 57–64.

Nishikawa, T., Akiyoshi, K., & Sunamoto, J. (1994). Supramolecular assembly between nanoparticles of hydrophobized polysaccharide and soluble-protein complexation between the self-aggregate of cholesterol-bearing pullulan and alpha-chymotrypsin. *Macromolecules*, *27*, 7654–7659.

Song, P. S., & Gordon, W. H. (1970). Spectroscopic study of excited states of coumarin. *Journal of Physical Chemistry*, *74*, 4234–4240.

Vieira, N. A. B., Moscardini, M. S., Tiera, V. A. D., & Tiera, M. J. (2003). Aggregation behavior of hydrophobically modified dextran in aqueous solution: A fluorescence probe study. *Carbohydrate Polymers*, *53*, 137–143.

Wagner, B. D. (2009). The use of coumarins as environmentally-sensitive fluorescent probes of heterogeneous inclusion systems. *Molecules*, *14*, 210–237.

Wondraczek, H., Elschner, T., & Heinze, T. (2011). Synthesis of highly functionalized dextran alkyl carbonates showing nanosphere formation. *Carbohydrate Polymers*, *83*, 1112–1118.

Wondraczek, H., & Heinze, T. (2008). Efficient synthesis and characterization of new photoactive dextran esters showing nanosphere formation. *Macromolecular Bioscience*, *8*, 606–614.

Yinsong, W., Lingrong, L., Jian, W., & Zhang, Q. (2007). Preparation and characterization of self-aggregated nanoparticles of cholesterol-modified o-carboxymethyl chitosan conjugates. *Carbohydrate Polymers*, *69*, 597–606.

Zatryb, G., Podhorodecki, A., Misiewicz, J., Cardin, J., & Gourbilleau, F. (2011). On the nature of the stretched exponential photoluminescence decay for silicon nanocrystals. *Nanoscale Research Letters*, *6*, 106.